ACKNOWLEDGMENTS

This work was supported by a Grant-in-Aid for Scientific Research on Priority Areas of the Japanese Ministry of Education, Science, Sports and Culture from the Ministry of Education, Science, Sports and Culture of Japan (contract grant numbers: 16022205 and 17014006), and by the 21st Century COE Program Special Research Grant "the Center for Innovative Therapeutic Development for Common Diseases" from the Ministry of Education, Science, Sports and Culture of Japan.

AUTHORSHIP AND CONFLICT OF INTEREST STATEMENTS

Hiroshi Kimura: performed research, wrote the paper, no conflict of interest

Hiroki Miyashita: prepared KO mice, no conflict of interest

Yasuhiro Suzuki: prepared KO mice, no conflict of interest

Miho Kobayashi: Transfection to MS1 cells, no conflict of interest

Kazuhide Watanabe: Analysis of the intracellular localization, no conflict of interest

Hikaru Sonoda: prepared antibodies, no conflict of interest

Hideki Ohta: prepared antibodies, no conflict of interest

Takashi Fujiwara: performed electron microscopy, no conflict of interest

Tooru Shimosegawa: designed the research, no conflict of interest

Yasufumi Sato: designed the research, wrote the paper, no conflict of interest

REFERENCES

1. Adams RH, Alitalo K. Molecular regulation of angiogenesis and lymphangiogenesis. Nat Rev Mol Cell Biol. 2007;8:464-478.
2. Sato Y. Update on endogenous inhibitors of angiogenesis. Endothelium. 2006;13:147-155.
3. Dawson DW, Volpert OV, Gillis P, Crawford SE, et al. Pigment epithelium-derived factor: a potent inhibitor of angiogenesis. Science. 1999;285:245-248.
4. Renno RZ, Youssri AI, Michaud N, Gragoudas ES, Miller JW. Expression of pigment epithelium-derived factor in experimental choroidal neovascularization. Invest Ophthalmol Vis Sci. 2002;43:1574-1580.
5. Hiraki Y, Inoue H, Iyama K, et al. Identification of chondromodulin I as a novel endothelial cell growth inhibitor. Purification and its localization in the avascular zone of epiphyseal cartilage. J Biol Chem. 1997;272:32419-32426.
6. Yoshioka M, Yuasa S, Matsumura K, et al. Chondromodulin-I maintains cardiac valvular function by preventing angiogenesis. Nat Med. 2006;12:1151-1159.
7. Zhang M, Volpert O, Shi YH, Bouck N. Maspin is an angiogenesis inhibitor. Nat Med. 2000;6:196-199.
8. Maass N, Nagasaki K, Ziebart M, Mundhenke C, Jonat W. Expression and

regulation of tumor suppressor gene maspin in breast cancer. Clin. Breast Cancer. 2002;3:281-287.

9. Kopp HG, Hooper AT, Broekman MJ, et al. Thrombospondins deployed by thrombopoietic cells determine angiogenic switch and extent of revascularization. J Clin Invest. 2006;116:3277-3291.

10. Kalluri R. Basement membranes: structure, assembly and role in tumour angiogenesis. Nat Rev Cancer. 2003;3:422-433.

11. Watanabe K, Hasegawa Y, Yamashita H, et al. Vasohibin as an endothelium-derived negative feedback regulator of angiogenesis. J Clin Invest. 2004;114:884-886.

12. Shimizu K, Watanabe K, Yamashita H, et al. Gene regulation of a novel angiogenesis inhibitor, vasohibin, in endothelial cells. Biochem Biophys Res Commun. 2005;327:700-7006.

13. Sonoda H, Ohta H, Watanabe K, Yamashita H, Kimura H, Sato Y. Multiple processing forms and their biological activities of a novel angiogenesis inhibitor vasohibin. Biochem Biophys Res Commun. 2006;342:640-646.

14. Shen JK, Yang XR, Sato Y, Campochiaro PA. Vasohibin is Up-regulated by VEGF in the Retina and Suppresses VEGF receptor 2 and Retinal Neovascularization. FASEB J. 2006;20:723-725.

15. Yamashita H, Abe M, Watanabe K, et al. Vasohibin prevents arterial neointimal formation through angiogenesis inhibition. Biochem Biophys Res Commun. 2006;345:919-925.

16. Shibuya T, Watanabe K, Yamashita H, et al. 2006. Isolation of vasohibin-2 as a sole homologue of VEGF-inducible endothelium-derived angiogenesis inhibitor vasohibin: a comparative study on their expressions. Arterioscler Thromb Vasc Biol. 26:1051-1057.

17. Sato Y, Sonoda H. The vasohibin family: a negative regulatory system of angiogenesis genetically programmed in endothelial cells. Arterioscler Thromb Vasc Biol. 2007;27:37-41.

18. Tepper OM, Capla JM, Galiano RD, et al. Adult vasculogenesis occurs through in situ recruitment, proliferation, and tubulization of circulating bone marrow-derived cells. Blood. 2005;105:1068-1077.

19. Oike Y, Akao M, Yasunaga K, et al. Angiopoietin-related growth factor antagonizes obesity and insulin resistance. Nat Med. 2005;11:400-408.

20. Yamazaki D, Suetsugu S, Miki H, et al. WAVE2 is required for directed cell migration and cardiovascular development. Nature. 2003;424:452-456.

21. Namba K, Abe M, Saito S, et al. Indispensable role of the transcription factor

PEBP2/CBF in angiogenic activity of a murine endothelial cell MSS31.Oncogene. 2000;19:106–114.

22. Rabbany SY, Heissig B, Hattori K, Rafii S. Molecular pathways regulating mobilization of marrow-derived stem cells for tissue revascularization. Trends Mol Med. 2003;9:109-117.

23. Barbera-Guillem E, Nyhus JK, Wolford CC, Friece CR, Sampsel JW. Vascular endothelial growth factor secretion by tumor-infiltrating macrophages essentially supports tumor angiogenesis, and IgG immune complexes potentiate the process. Cancer Res. 2002;62:7042-7049.

24. Cho CH, Koh YJ, Han J, et al. Angiogenic role of LYVE-1-positive macrophages in adipose tissue. Circ Res. 2007;100:e47-57.

25. Shutter JR, Scully S, Fan W, et al. Dll4, a novel Notch ligand expressed in arterial endothelium. Genes Dev. 2000;14:1313-1318.

26. Duarte A, Hirashima M, Benedito R, et al. Dosage-sensitive requirement for mouse Dll4 in artery development. Genes Dev. 2004;18:2474-2478.

27. Williams CK, Li JL, Murga M, Harris AL, Tosato G. Up-regulation of the Notch ligand Delta-like 4 inhibits VEGF-induced endothelial cell function. Blood. 2006;107:931-939.

28. Hellstrom M, Phng LK, Hofmann JJ, et al. Dll4 signalling through Notch1 regulates formation of tip cells during angiogenesis. Nature. 2007;445:776-780.

29. Siekmann AF, Lawson ND. Notch signalling limits angiogenic cell behaviour in developing zebrafish arteries. Nature. 2007;445:781-784.

30. Leslie JD, Ariza-McNaughton L, Bermange AL, McAdow R, Johnson SL, Lewis J. Endothelial signaling by the Notch ligand Delta-like 4 restricts angiogenesis. Development. 2007;134:839-844.

31. Lobov IB, Renard RA, Papadopoulos NJ, et al. Delta-like ligand 4 (Dll4) is induced by VEGF as a negative regulator of angiogenic sprouting. Proc Natl Acad Sci USA. 2007;104:3219-3224.

32. Noguera-Troise I, Daly C, Papadopoulos NJ, et al. Blockade of Dll4 inhibits tumour growth by promoting non-productive angiogenesis. Nature. 2006;444:1032-1037.

33. Ridgway J, Zhang G, Wu Y, et al. Inhibition of Dll4 signalling inhibits tumour growth by deregulating angiogenesis. Nature. 2006;444:1083-1087.

FIGURE LEGENDS

Fig. 1: New vessel distribution in the skin flap.

A: The vascular distribution in the skin flap was observed in areas every 2 mm interval from the necrotic edge. CD31 (red) is a marker for ECs, and αSMA (green) is a marker for mural cells. Scale bars are 200 μm. **B:** The dashed line indicates the necrotic edge. The vascular area and vascular density per high power field were determined from every 2 mm interval from the necrotic edge. Data are expressed as the means and SDs of each area.

Fig. 2: The spatio-temporal expression profile of VASH1.

A: Immunostaining of CD31 (red), αSMA (green), PCNA (green), and/or VASH1 (green) was performed using the indicated area of the skin flap. **B:** Total RNA was isolated from each area of the skin flap. Quantitative real time RT-PCR was performed to show mRNA levels of VASH1 in each area. Each value was standardized with β-actin. **C:** HUVECs of sparse, subconfluent and confluent conditions were treated with or without VEGF (1 nM) for 12 h, and the expression of VASH1 was determined by Northern blotting.

Fig. 3: The spatio-temporal expression profile of VASH2.

A: Immunostaining of VASH2, CD11b and F4/80 in the area 0-2 mm from the necrotic edge. Scale bars are 200 μm. **B:** Total RNA was isolated from each area of the skin flap. Quantitative real time RT-PCR was performed to show mRNA levels of VASH2 in each area. Each value was standardized with β-actin. **C:** The basal level of VASH2 mRNA in HUVECs or THP-1 cells was determined by RT-PCR. **D:** After confirming bone marrow reconstitution, the subcutaneous angiogenesis experiment was performed. Immunostaining of VASH2 in the area 0-2 mm from the necrotic edge is shown. Arrow heads indicate GFP positive and VASH2 positive cells. Scale bar is 50 μm.

Fig. 4: Effects of exogenous VASH1 or VASH2 on angiogenesis in the skin flap

AdVASH1 or AdVASH2 was injected into the tail vein to supply sufficient exogenous proteins to the site of angiogenesis. **A:** Immunostaining of CD31 (red) and αSMA (green) positive cells in the indicated area of the skin flap. Scale bars are 50 μm. **B:** Vascular area was determined from 5 different fields in each area. Data are expressed as the means and SDs. *$p<0.01$, **$p<0.05$.

Fig. 5: Generation of *VASH1* and *VASH2* knockout mice and their steady-state

subcutaneous vascular architecture

A: *VASH1* and *VASH2* knockout mice were generated as described in Materials and Methods. Genotyping and the analysis of each transcript by RT-PCR were shown. **B:** Ear skin was used to show the steady-state vascular architecture of ear skin. Upper panels show immunostaining of CD31 (green) and LYVE-1 (red). Lower panels show SEM of capillary vessels.

Fig. 6: Vascular distribution in the skin flap of *VASH1* knockout mice

VASH1 knockout mice were applied to the model of subcutaneous angiogenesis. **A:** Immunostaining of CD31 (red) and αSMA (green) in the area 6-8 mm from the necrotic edge is shown. Scale bars are 200 μm. **B:** The vascular area was determined from 5 different fields in each area. Data are expressed as the means and SDs. *$p<0.01$, **$p<0.05$. **C:** Lectin staining (green) shows the perfusion of new vessels in the area 6-8 mm from the necrotic edge. The same section was immunostained for CD31 (red). Scale bars are 200 μm. **D:** Adenoviral-mediated gene transfer was performed to supplement the deficient protein in *VASH1* knockout mice. AdLacZ was use as the control. Immunostaining of CD31 (red) and αSMA (green) in the indicated area of the skin flap is shown. Scale bars are 200 μm.

Fig. 7: Vascular distribution in the skin flap of *VASH2* knockout mice

VASH2 knockout mice were applied to the model of subcutaneous angiogenesis. **A:** Immunostaining of CD31 (red) and αSMA (green) in the area 2-4 mm from the necrotic edge is shown. Scale bars are 200 μm. **B:** The vascular area was determined from 5 different fields in each area. Data is expressed as the means and SDs. *$p<0.01$, **$p<0.05$. **C:** Immunostaining of CD11b (red) in the area 0-2 mm from the necrotic edge is shown in wild-type and *VASH2* (-/-) mice. Scale bars are 200 μm. **D:** Adenoviral-mediated gene transfer was performed to supplement the deficient protein in *VASH2* knockout mice. AdLacZ was use as the control. Immunostaining of CD31 (red) and αSMA (green) in the indicated area of the skin flap is shown. Scale bars are 200 μm.

Figure 1. Kimura et al

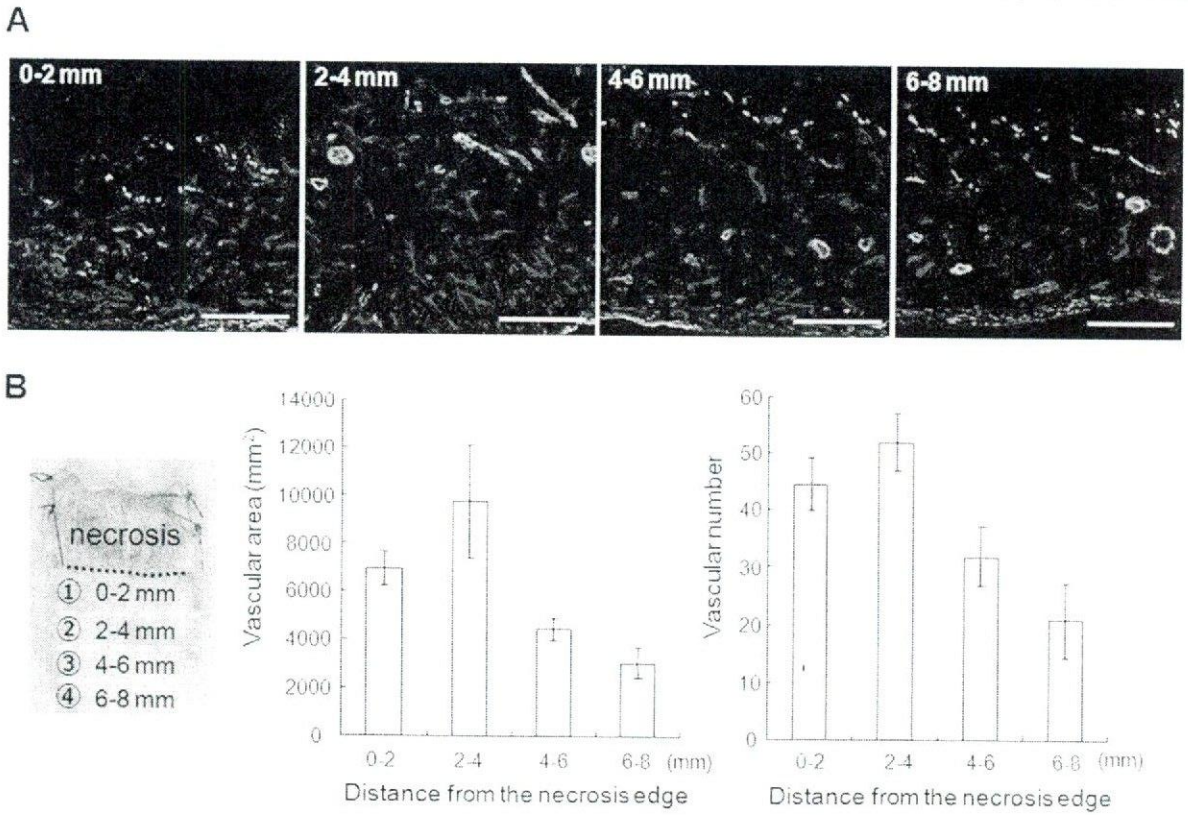

Figure 2 Kimura et al

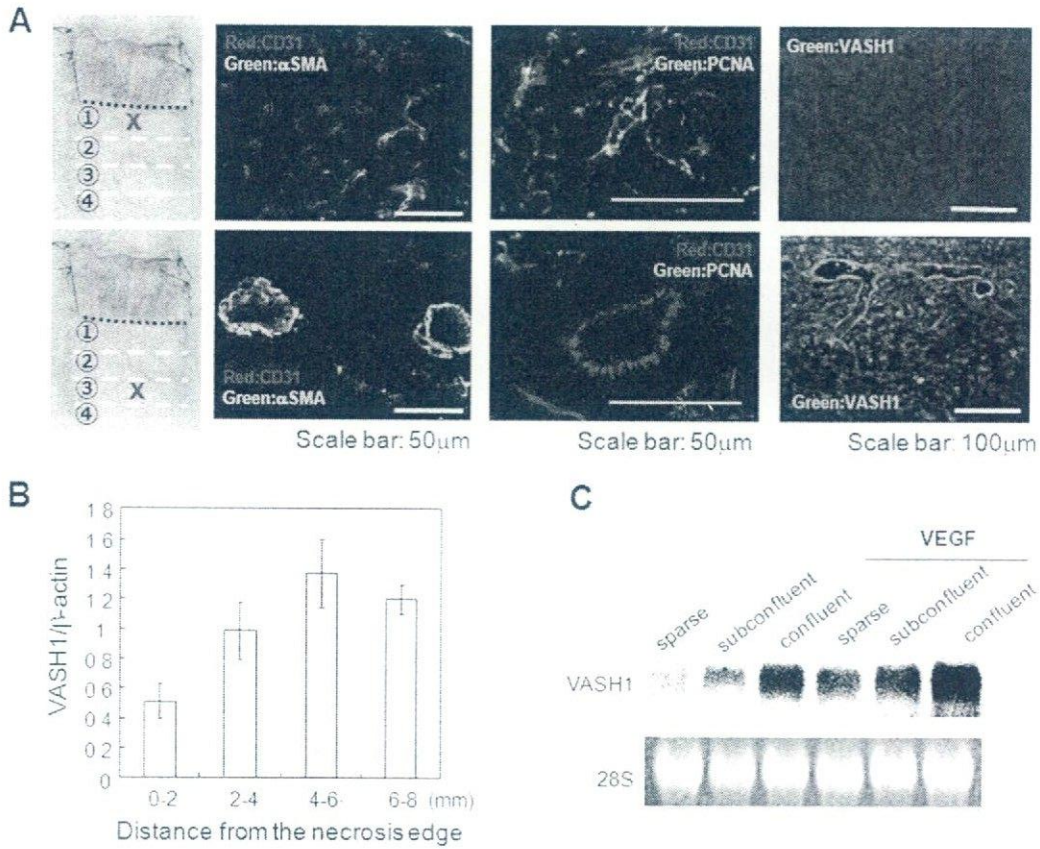

Figure 3. Kimura et al

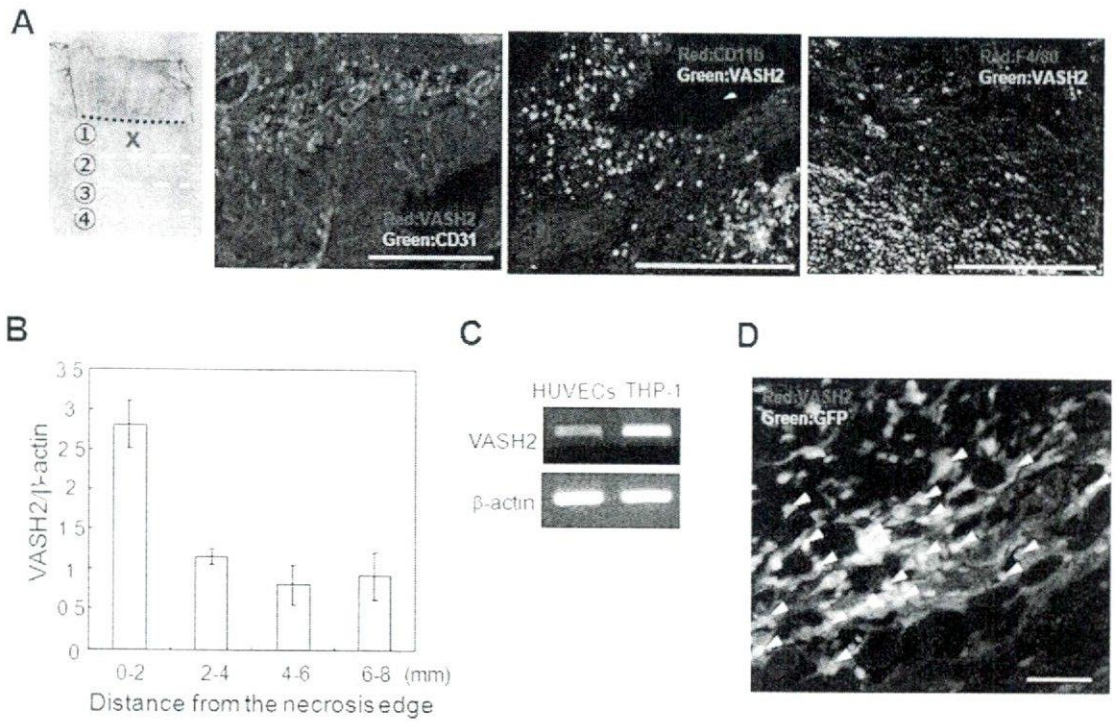

Figure 4. Kimura et al

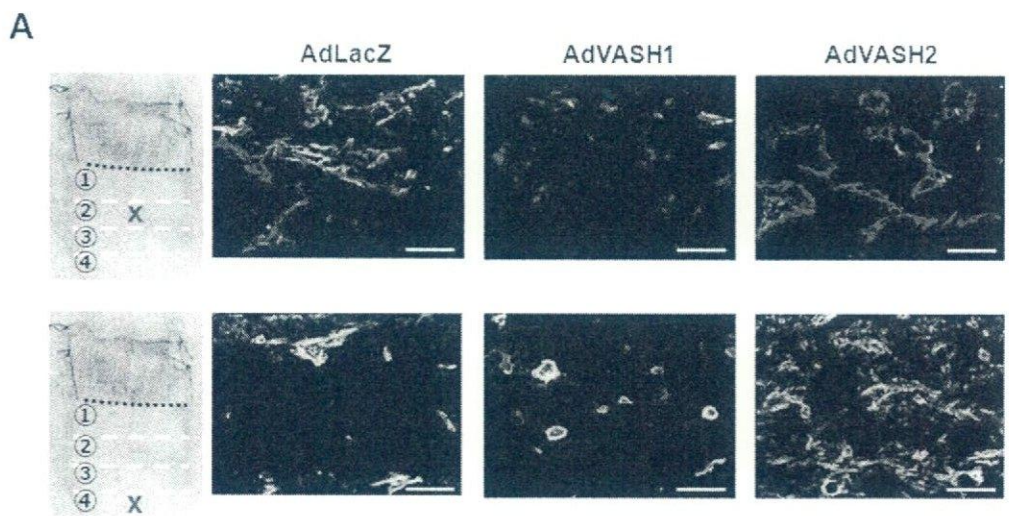

Figure 4 Kimura et al

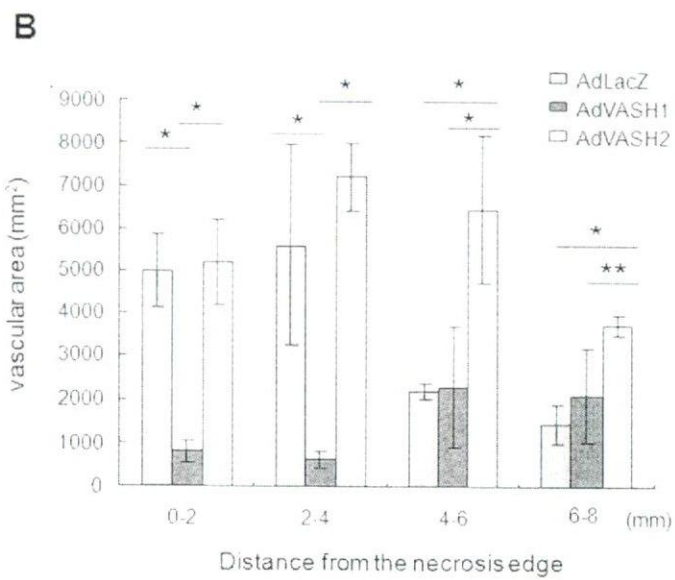

Figure 5. Kimura et al

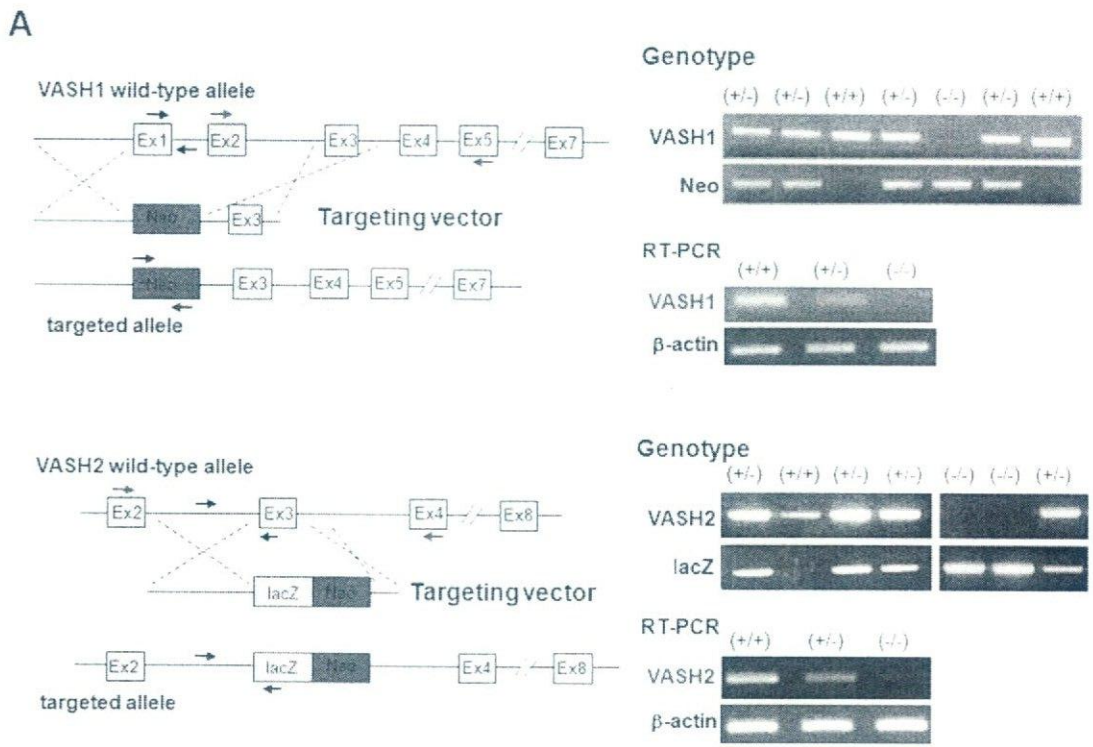

Figure 5 Kimura et al

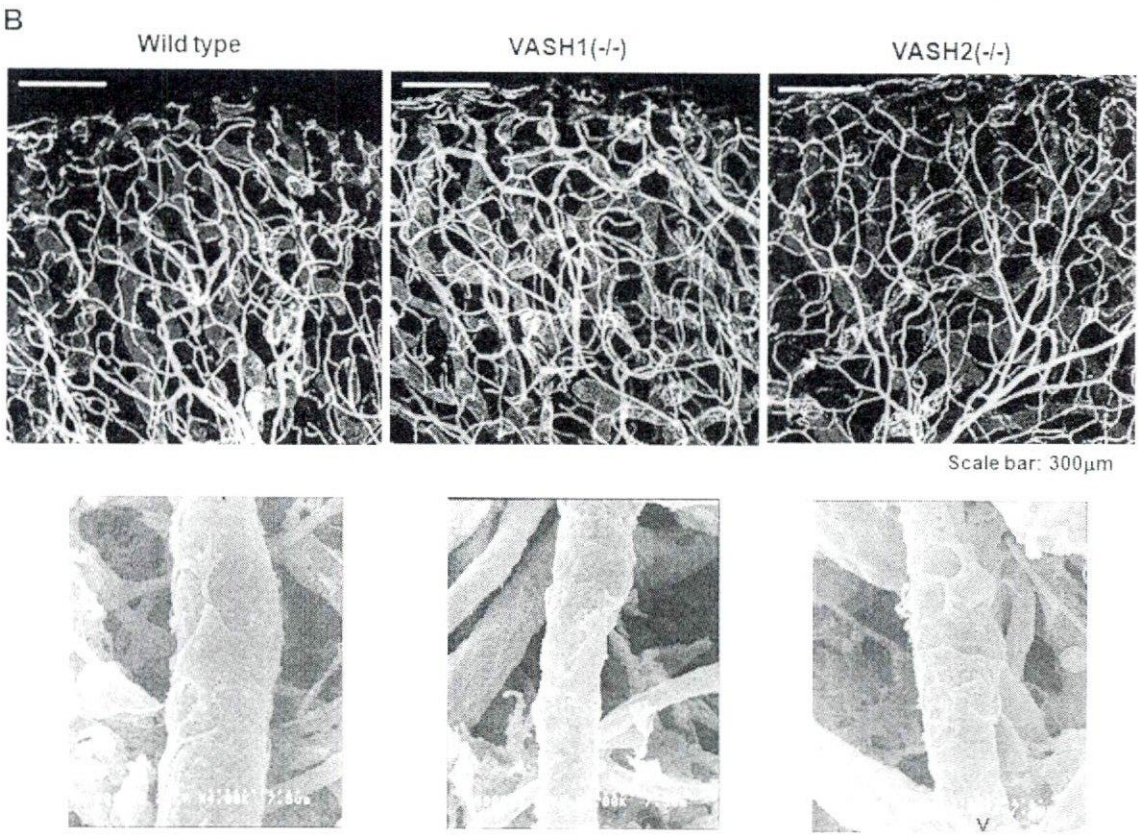

Figure 6. Kimura et al

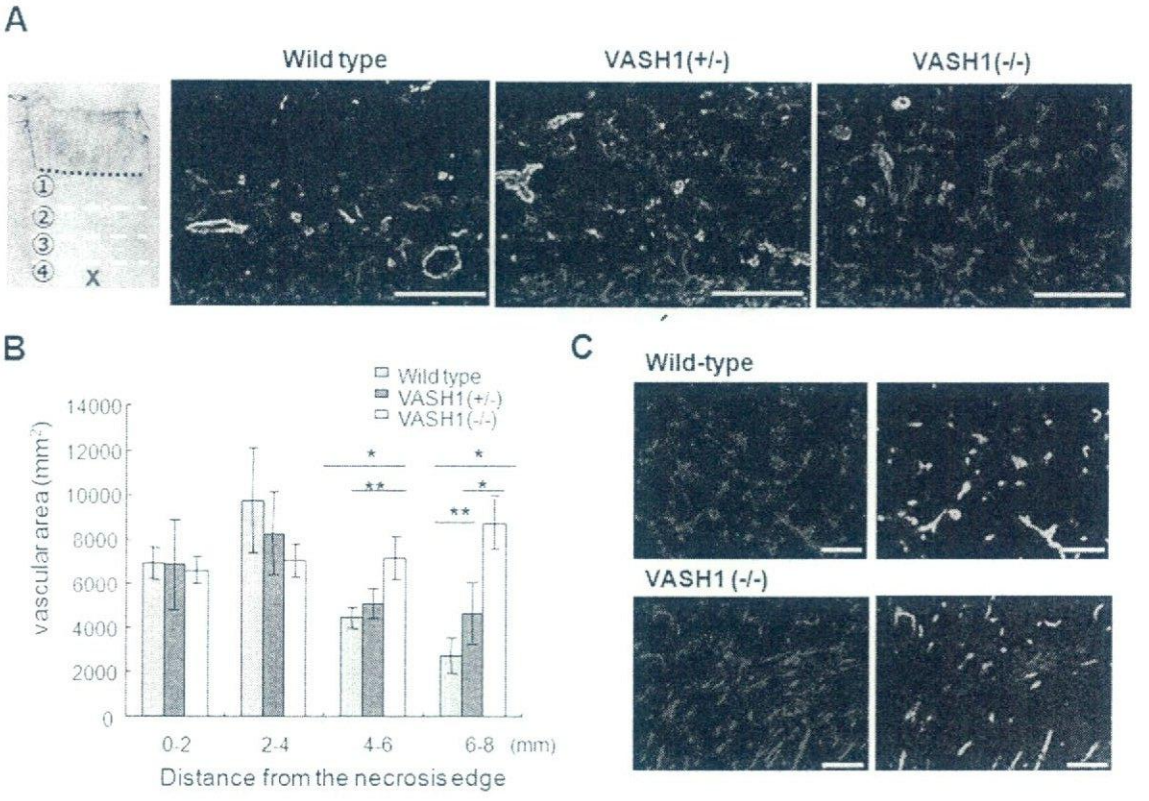

Figure 6. Kimura et al